Dynamic Isomerization of a Supramolecular Tetrahedral M_4L_6 Cluster[1]

Thomas Beissel, Ryan E. Powers, Tatjana N. Parac, and Kenneth N. Raymond*

Contribution from the Department of Chemistry, University of California, Berkeley, California 94720

Received November 23, 1998. Revised Manuscript Received March 4, 1999

Abstract: The bis-hydroxamate ligand isophthal-di-*N*-(4-methylphenyl)hydroxamate (**E**) forms tetrahedral clusters of the type $M_4\mathbf{E}_6$ (M = Ga(III), Fe(III)). The syntheses of these and several other tetrahedral metal clusters have illustrated a general approach to the design of supramolecular metal clusters based on incommensurate coordination number interactions. In each case, rigid spacers separate bidentate units and preclude formation of metal coordination species other than the one targeted. For the $Ga_4\mathbf{E}_6$ cluster described here each vertex is a chiral metal center (Δ or Λ) that generates clusters with *T* (ΔΔΔΔ or ΛΛΛΛ), C_3 (ΔΔΔΛ or ΛΛΛΔ), or S_4 (ΔΔΛΛ) symmetry. The rigid ligand spacer is bimodal, accommodating either mixed or homochiral metal centers at either end, but locks in the chirality of the complex once formed. Therefore all three isomers are seen in solution and their interconversion, although still on the NMR time scale, is significantly slower than isomerization of similar unimolecular hydroxamate complexes. The distribution of the isomers in aqueous solution for the *T*, C_3, and S_4 isomers is 4, 58, and 38%, respectively. The barrier to the interconversions, which occur through a nondissociative trigonal twist at the metal centers, is 58 kJ mol^{-1} for each of the isomerization steps. The syntheses of the ligand and corresponding iron and gallium complexes are described. The compound $Ga_4\mathbf{E}_6$·18 DMF (DMF = dimethylformamide) crystallizes in $I4_1/a$ with $Z = 8$, $a = 24.0738(2)$ Å, and $c = 68.5828(5)$ Å. Full-matrix refinement of data collected on a CCD detector with 7710 observations and 576 variables gave an *R* factor (on *F*) of 0.089. Two crystallographically independent clusters are chemically equivalent, both lying on $\bar{4}$ special positions. The Ga-to-Ga distances between metal centers with like and opposite chiralities are 9.0 and 8.8 Å, respectively. Two different ligand conformations are observed: one bridging homochiral metal centers and the other mixed chiral centers. Their nearly equal stability explains the mix (*T*, C_3, S_4) of cluster isomers seen. This ligand couples the metal vertices in the cluster so as to increase significantly the transition state free energy for Λ−Δ interconversion but does not couple the chirality for the Λ or Δ ground state.

Introduction

Molecular materials are increasingly being prepared by design, using metal−ligand bonds to make ordered assemblies. Spectacular structures can result from such assemblies. There are examples of squares,[2−5] grids,[6,7] and three-dimensional metal arrays.[8−10] Tetrahedral clusters have been synthesized using both monodentate[2,11] and bidentate ligands[12−14] to provide the necessary linkages.

In contrast to kinetically inert materials whose structures are fixed at the time of synthesis, the supramolecular structures found in nature are dynamic and typically on the nanometer scale. We have described a model for the highly symmetrical supramolecular structures of ferritin and protein viral coats that explains the high symmetry (octahedral for the 24-mer ferritin and icosahedral for the 60-mer protein viral coat, respectively) of these protein clusters as due to incommensurate coordination numbers at the interaction sites of the monomers.[15−19] Such noncovalently linked assembly requires a driving force and a dynamic equilibrium in formation, since the unique high-

(1) This paper is paper number 8 in the series "Coordination Number Incommensurate Cluster Formation". For the previous paper, see ref 20.

(2) Fujita, M.; Oguro, D.; Miyazawa, M.; Oka, H.; Yamaguchi, K.; Ogura, K. *Nature* **1995**, *378*, 469.

(3) Stang, P. J.; Olenyuk, B. *Acc. Chem. Res.* **1997**, *30*, 502.

(4) Stang, P. J.; Cao, D. H.; Saito, S.; Arif, A. M. *J. Am. Chem. Soc.* **1995**, *117*, 6273.

(5) Olenyuk, B.; Whiteford, J. A.; Stang, P. J. *J. Am. Chem. Soc.* **1996**, *118*.

(6) Youinou, M. T.; Rahmouni, N.; Fisher, J.; Osborn, J. A. *Angew. Chem., Int. Ed. Engl.* **1992**, *31*, 733.

(7) Baxter, P.; Lehn, J. M.; Fisher, J.; Youinou, M. T. *Angew. Chem., Int. Ed. Engl.* **1994**, *33*, 2284.

(8) Baxter, P.; Lehn, J. M.; DeCian, A.; Fisher, J. *Angew. Chem., Int. Ed. Engl.* **1993**, *32*, 69.

(9) Hanan, G. S.; Arana, C. R.; Lehn, J. M.; Fenske, D. *Angew. Chem., Int. Ed. Engl.* **1995**, *34*, 1122.

(10) Saalfrank, R. W.; Burak, R.; Reihs, S.; Low, N.; Hampel, F.; Stachel, H.; Lentmaier, J.; Peters, K.; Peters, E.; Georg von Schnering, H. *Angew. Chem., Int. Ed. Engl.* **1995**, *34*, 993.

(11) Mann, S.; Huttner, G.; Laszlo, Z.; Heinze, K. *Angew. Chem., Int. Ed. Engl.* **1996**, *35*, 2808.

(12) Saalfrank, R. W.; Horner, B.; Stalke, D.; Salbeck, J. *Angew. Chem., Int. Ed. Engl.* **1993**, *32*, 1179.

(13) Saalfrank, R. W.; Burak, R.; Breit, A.; Stalke, D.; Herbst-Irmer, R.; Daub, J.; Porsch, M.; Bill, E.; Muther, M.; Trautwein, A. X. *Angew. Chem., Int. Ed. Engl.* **1994**, *33*, 1621.

(14) Amoroso, A. J.; Jeffery, J. C.; Jones, P. L.; McClevery, J. A.; Thornton, P.; Ward, M. D. *Angew. Chem., Int. Ed. Engl.* **1995**, *34*, 1443.

(15) Beissel, T.; Powers, R. E.; Raymond, K. N. *Angew. Chem., Int. Ed. Engl.* **1996**, *35*, 1084.

(16) Raymond, K. N.; Caulder, D. L.; Powers, R. E.; Beissel, T.; Meyer, M.; Kersting, B. *Proc. Robert A. Welch Found. Conf. Chem. Res.* **1996**, *40*, 115.

(17) Caulder, D. L.; Raymond, K. N. *Angew. Chem., Int. Ed. Engl.* **1997**, *36*, 1439.

(18) Brückner, C.; Powers, R. E.; Raymond, K. N. *Angew. Chem., Int. Ed.* **1998**, *37*, 1837.

(19) Caulder, D. L.; Powers, R. E.; Parac, T. N.; Raymond, K. N. *Angew. Chem., Int. Ed. Engl.* **1998**, *37*, 1840.
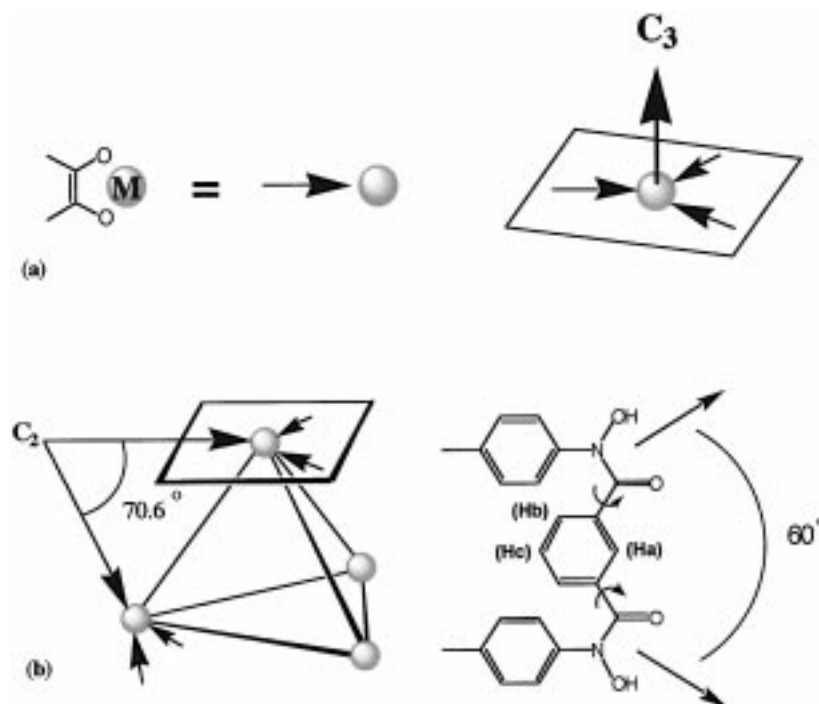
Figure 1. (a) In this approach to cluster design, the bidentate ligand is regarded as a *coordinate vector*. Multiple chelators on a single octahedral metal center must be arranged on the plane normal to the major axis (C_3) of the complex, represented by the bold arrow here. This plane is defined as a *coordinate plane*. (b) Each metal (represented by shaded spheres) lies in a plane generated by the three coordinating groups. These four "coordinate planes" of the tetrahedron meet at the C_2 axis at an angle of 70.6°. In order for the cluster to form, the coordinate vectors of the individual ligands must lie in these planes. The arrows represent "coordinate vectors". In the bis-hydroxamate ligand's planar form these vectors are 60° apart. To form the M₄L₆ cluster the ligand must rotate the two bonds (highlighted with circular arrows) to increase this angle to about 70.6°.

symmetry product is the most thermodynamically stable. This model predicts a rational basis for the design of supramolecular clusters. These clusters employ fewer, but stronger, metal−ligand coordinate bonds than the many weak interactions composed of hydrogen bonds and van der Waals interactions along large regions or surfaces for protein−protein interactions. Because metal−ligand coordinate bonds are highly directional and much stronger than hydrogen bonds or van der Waals contacts, a small number can be used to direct cluster formation. We have demonstrated the utility and generality of this approach in the synthesis of M₂L₃ triple helicates,[17] M₄L₆ edge-bridged tetrahedra,[15,19] and M₄L₄ face-bridged tetrahedra.[18]

The M₄L₆ clusters described in this paper were designed to have tetrahedral symmetry, as characterized by incommensurate 3-fold and 2-fold symmetry axes (Figure 1). The 3-fold axis is formed when three bidentate chelating groups coordinate an "octahedral" metal ion. The ligand is designed to have 2-fold symmetry, with two rigidly separated bidentate hydroxamate groups. By defining the targeted cluster as a polyhedron consisting of planes normal to the 3-fold axes of the individual metal centers, the required ligand design parameters can be derived.[16] "Coordinate vectors" are defined that bisect the individual coordinating chelators (Figure 1a). To form a M₄L₆ tetrahedron the four metal complexes must have an angle of 70.6° between any two chelate planes at the 2-fold axis (Figure 1b). If other stoichiometries and geometries are precluded, only the M₄L₆ tetrahedron can form.

This expectation was fulfilled in the formation of the complex described here, which is a discrete tetramer in solution, the solid state, and gas phase, but exists in any of three point group symmetries. This is because each of the four cluster vertices is chiral. There are four metal stereo centers that can (in principle) form three different complexes, two of which are racemic pairs. As described in a preliminary report[15] the Ga₄**E**₆ (**E** = isophthal-

di-*N*-(4-methylphenyl)hydroxamate) cluster crystallizes with S_4 symmetry, with ΔΔΔΔ chirality at the metal centers.

We have since shown[17] that a similar, rigid, naphthyl-linked bis-catechol complex M₄**L**₆ (M = Ga(III), Fe(III), **L** = 1,5-bis(2,3- dihydroxybenzamido)naphthalene) contains clusters with homochiral metal centers, i.e., only ΔΔΔΔ and ΛΛΛΛ complexes are formed. The naphthyl clusters have cavities large enough to form host−guest complexes, and the solution NMR spectra of the guests display the chiral environment of the host cluster.[20] In another example, a smaller catechol cluster is formed from a chiral ligand, which makes each metal center homochiral.[21]

As noted, our design principles have also been applied to two-vertex systems to generate helicates.[17,22] The first such triple-stranded helicate fully structurally characterized was an Fe₂L₃ complex in which L is a dihydroxypyridonate bridged by flexible linkers.[23] To fully control helicate formation a bridged linker is required; the chirality at one metal center in such a complex enforces a chiral preference at the second metal center through mechanical coupling, which is what selects for the helix form over other geometries.[24,25] While there had been much discussion and speculation about this interaction, until recently, there were no data to measure it. The magnitude of the chiral center interaction was determined in a series of predesigned dinuclear triple-stranded helicates formed from rigid

(20) Parac, T. N.; Caulder, D. L.; Raymond, K. N. *J. Am. Chem. Soc.* **1998**, *120*, 8003.

(21) Enemark, E. J.; Stack, T. D. P. *Angew. Chem., Int. Ed. Engl.* **1998**, *37*, 932.
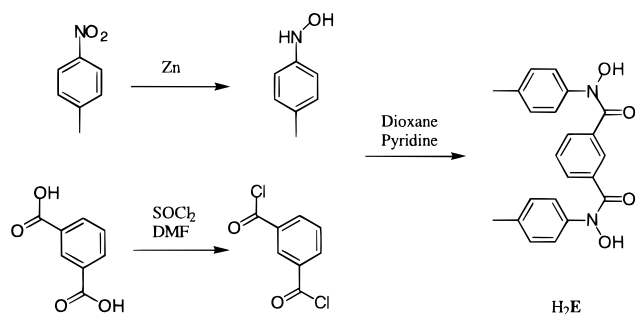
(22) Kersting, B.; Meyer, M.; Powers, R. E.; Raymond, K. N. *J. Am. Chem. Soc.* **1996**, *118*, 7221.

(23) Scarrow, R. C.; White, D. L.; Raymond, K. N. *J. Am. Chem. Soc.* **1985**, *107*, 6540.

(24) Piguet, C.; Bernardinelli, G.; Hopfgartner, G. *Chem. Rev.* **1997**, *97*, 2005.

(25) Williams, A. *J. Chem. Eur.* **1997**, *3*, 3.

Scheme 1

phenylene-bridged bis-terephthalamide catecholate ligands and their gallium(III) complexes.[22] Inversion of the dinuclear Ga_2L_3 helicates occurs on the NMR time scale and proceeds through an intramolecular Bailar twist. Chirality of the two metal ion sites is weakly coupled, such that the heterochiral (Λ,Δ) form of the cluster only appears as a kinetic intermediate. The energy of this intermediate gives a measure of the mechanical coupling between the two metal vertices.

A major goal of this paper is to examine the mechanical coupling between the vertices of a tetrahedral cluster. As with the helicate system we address the problem using variable-temperature NMR studies so that the kinetic barrier for the $\Lambda \leftrightarrow \Delta$ interconversion provides an estimate of the mechanical coupling between the metal centers. This analysis is accompanied by the full description of the synthesis, characterization, and solid-state structure of the M_4E_6 complexes (M = Fe, Ga).

Results and Discussion

Synthesis and Characterization. The ligand H_2E, shown in Scheme 1 was prepared through the reaction of isophthaloyl dichloride with *N*-(4-methylphenyl)hydroxylamine (prepared through the reduction of 4-nitrotoluene with zinc under neutral conditions). Solutions of $Fe(acac)_3$ or $Ga(acac)_3$ in methanol (acac = acetyl acetonate) were added to a solution of the ligand with a few drops of triethylamine in acetone to yield red or colorless microcrystalline precipitates of Fe_4E_6 or Ga_4E_6, respectively.

Both complexes showed intense peaks for the molecular mass of the tetrahedral clusters in the FAB$^+$ mass spectrum. No higher mass ions were observed. The UV/vis spectrum of Fe_4E_6 shows a strong absorption at 440 nm, which is typical of a tris-hydroxamato iron(III) complex. The molar intensity (per Fe) of this charge-transfer band is 3780 $M^{-1}cm^{-1}$, near the value that is observed for the mononuclear tris(benzohydroxamato)-iron(III) complex.[26]

The ^1H NMR spectrum of H_2E shows a pattern that is in accord with its 2-fold symmetry. The ^1H NMR spectrum of the tetrahedral gallium cluster was taken in CD_2Cl_2 and demonstrated the same splitting pattern that is observed for the free ligand. Solutions containing an excess of ligand only showed signals for the cluster and the free ligand. The lack of mixed complexes demonstrates the cooperative assembly of the system. The absence of exchange between the bound and unbound ligands on the NMR time scale shows the stability and integrity of the complex on this time scale.

Differences are seen between the proton chemical shifts of the bound and unbound ligand. The protons on the toluene groups (which point out from the surface of the cluster) are essentially in the same chemical environment as in the free

ligand, and these signals show minimal difference in the chemical shift (0.06−0.14 ppm) compared to the free ligand. Larger differences are found for the peaks corresponding to the aromatic protons of the linker units of the ligand. The three protons adjacent to each other, resulting in a doublet "H_b" and a triplet "H_c" (Figure 1b), are expected to be in contact with the solvent on the exterior of the cluster. The resulting downfield shift in the signals that correspond to these protons is relatively small (0.25−0.41 ppm). The remaining single proton of the backbone, H_a, points into the cluster cavity and is therefore in a significantly different environment than the analogous proton in the free ligand. Consequently, this proton exhibits the largest downfield chemical shift (1.26 ppm compared to the free ligand) and it is broadened considerably at room temperature.

The cyclic voltammetry of the Fe_4E_6 cluster (in acetonitrile solvent with tertiary butylammonium hexafluorophosphate, 0.1 M, as electrolyte) shows a quasi-reversible reduction at −1.3 V vs ferrocene (Fc^+/Fc). The reduction and oxidation peaks are broadened, which is a sign that more than one metal center is involved. The peak-to-peak separation is 180 mV at a scan rate of 200 mV/s. Similar behavior was reported for a tetrahedral iron cluster by Saalfrank and co-workers.[27]

Solid-State Structure Analysis. The solid-state structure of the gallium cluster, Ga_4E_6, contains two crystallographically independent clusters, each of which lies on a special position with $\bar{4}$ (S_4) symmetry, a subgroup of T_d. The four metal ions are separated by an average of 8.9 Å. A space-filling picture of one of these nearly identical cluster structures is shown in Figure 2a. The approach angle of 31° corresponds to an average twist angle of 48°, typical for gallium hydroxamate structures.[28] The cluster has a relatively open, rigid cavity, which is partially filled with four crystallographically identical DMF molecules (Figure 2b). The average carbon-to-carbon distance between the DMF methyl groups within the cluster cavity is 4.0 Å, at van der Waals contact.

Figure 3 shows (at top) the two independent ligands in one of the M_4E_6 clusters. The gallium-to-gallium distances between metal centers with like and opposite chiralities are 9.0 and 8.8 Å, respectively. Figure 3 (at bottom) shows the Ga_4E_6 cluster represented as coordination planes. The metal ions are represented as spheres within each plane. The left side of the figure represents the ligand bridging metals of the *same* chirality. The coordinate vectors are shown to demonstrate how each ligand must twist to maintain the vectors within the planes. The only difference between this ligand form and the ligand bridging two metals of *opposite* chirality (Figure 3, right) is the relative direction of the torsion angles around the aromatic linker and the carbonyl group of each ligand arm. These bond rotations are all that is needed to accommodate the two different ligand forms, implying weak coupling of chirality between metal centers. That is, this rigid ligand is bimodal in the four metal cluster: it can accommodate equally either Λ or Δ chirality at one end when the chirality at the other end is fixed.

Variable-Temperature NMR of Ga_4T_6. The ^1H NMR spectrum of the gallium cluster was measured in 20 K intervals between room temperature and 220 K (Figure 4). With decreasing temperature the broad signal of the proton H_a splits into five distinct peaks at 9.10, 9.04, 8.99, 8.78, and 8.73 ppm. Integration of the intensities of these resonances at 220 K yields a ratio of 7:16:2:14:16, respectively.

(26) Abu-Dari, K.; Raymond, K. N. *J. Am. Chem. Soc.* **1977**, *99*, 2003.

(27) Saalfrank, R. W.; Burak, R.; Breit, A.; Stalke, D.; Herbst-Irmer, R.; Daub, J.; Porsch, M.; Bill, E.; Muther, M.; Trautwein, A. X. *Angew. Chem., Int. Ed. Engl.* **1994**, *33*, 1621.

(28) Borgias, B. A.; Barclay, S. J.; Raymond, K. N. *J. Coord. Chem.* **1986**, *15*, 109.
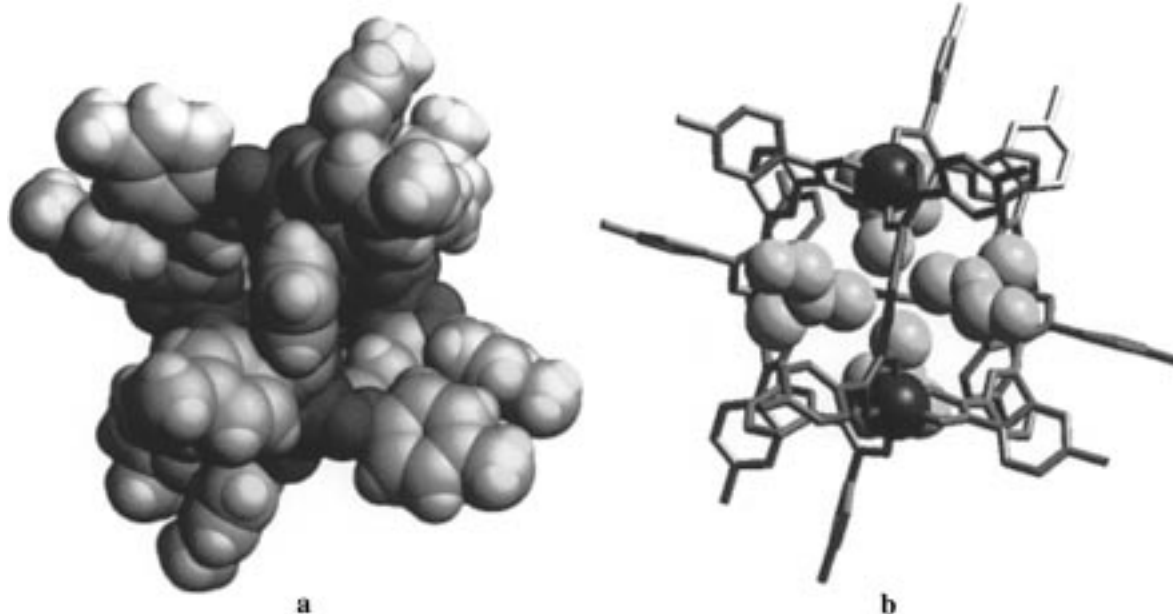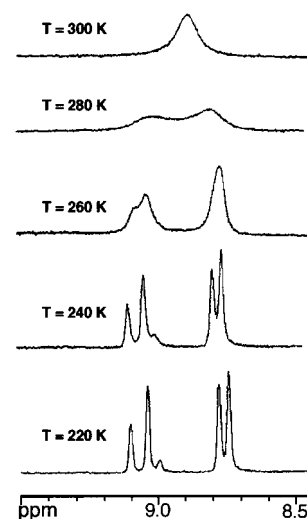
Figure 2. (a) Space-filling model of the crystal structure of the Ga_4E_6 cluster as viewed down the S_4 axis. (b) Crystal structure of Ga_4E_6 cluster. The ligand is shown in stick outline with space-filling representation of the four symmetry-related DMF molecules that fill the interior of the cluster. Hydrogen atoms are removed for clarity.
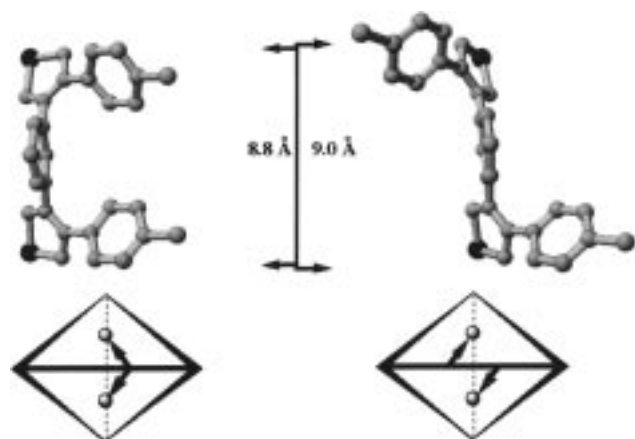
Figure 3. (top) Structure of two crystallographically independent ligands in the solid-state structure of the Ga_4E_6 cluster. On the left side is the ligand that bridges metal centers of the opposing chirality. On the right side is the ligand that chelates metals of the same chirality. (bottom) Ga_4E_6 cluster represented as chelate planes and spheres representing metal ions that center each plane. The chelate vectors for the two ligands above are included to demonstrate how each of the ligands must twist to maintain the vectors within the planes.


Figure 4. Variable-temperature ^1H NMR resonance of the "H_a" proton of the Ga_4E_6 cluster. At room temperature a single broad peak is observed. As the sample cools, this peak resolves into five signals which correspond to each of the possible hydrogen environments generated by all of the stereoisomers of the cluster.

The source of this isomerism is the chirality of the four tris-hydroxamate metal centers, which are Δ or Λ. The combination of these different chiralities leads to three possible isomers plus their enantiomers (Figure 5). The isomers where all four sites are homochiral leads to the highest possible symmetry, T, in which case one signal for the H_a protons is expected (the two enantiomers are magnetically equivalent.) The signal at 8.99 ppm corresponds to this isomer. Combining one center of either Δ or Λ configuration with three centers of opposite chirality leads to C_3 symmetry. Here the six H_a protons of each cluster are split into two groups of three: three that are on ligands coordinated to metal centers of different chirality and three on ligands that span metal centers of the same chirality. The two peaks at 9.04 and 8.73 ppm share the same integration and are assigned to this isomer. The third isomer is not chiral (S_4

symmetry), with two Δ and two Λ configuration metal centers. The six H_a protons in this isomer are split into two groups in the ratio of 2:4: the two protons on the ligands that connect metals of identical chirality and the remaining four on the ligands between complexes of opposite chirality. The remaining two peaks at 9.10 and 8.78 ppm with an integration of 7 and 14 correspond to this isomer.

Since the ^1H NMR spectrum shows the expected five peaks at 220 K, it is clear that all species are present in solution. If the distribution between the isomers were purely statistical, the relative amounts of $T:C_3:S_4$ are expected to be 12.5:50:37.5%. The integration of the peaks at 220 K gives the distribution of the $T:C_3:S_4$ isomers as 4:58:38%. Although the isomers are not present in exact statistical distribution, the distribution shows that the stability of the three isomers is very similar and therefore
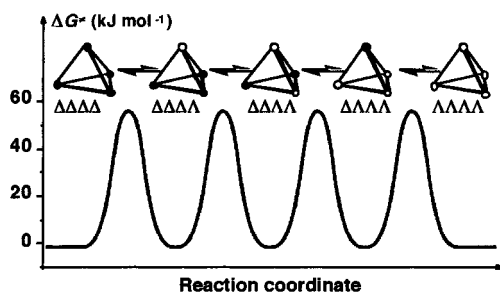
Figure 5. Stereochemical course and potential energy diagram for intramolecular inversion of the Ga₄T₆ cluster isomers. The individual isomers are identified by the chirality at the metal centers and the overall symmetry of the cluster. Metal complexes with Δ or Λ chirality are represented by darkly or lightly shaded spheres, respectively. The *T* symmetry cluster provides only one ligand environment. The S_4 and C_3 symmetry clusters provide two ligand environments in the ratios 1:2 and 1:1, respectively.

mechanical coupling between metal centers of opposite chirality is negligibly small for the ground-state complexes.

Using the CAChe system,[29] MM2 calculations were carried out using the structure of the gallium complex. These calculations provide a qualitative understanding of the various conformations of the supramolecular assembly and have been found to be invaluable as a means of discovering steric and bond strain problems in ligand design.[15−19] The calculations indicate that there is no significant energy difference between the three possible cluster symmetries. There is, however, a barrier to the transition state for Λ,Δ interconversion at each vertex.

Dynamic Behavior of Ga₄T₆. Hydroximato- and hydroxamatoiron(III) complexes have been resolved in acetone solutions,[26] showing that in this solvent isomerization is extremely slow. However, in weakly acidic aqueous and alcoholic solutions, these complexes racemize immediately. Ligand exchange in hexadentate hydroxamate iron(III) complexes has been previously studied by NMR,[30] but isomerization of a simple tris-hydroxamate iron(III) or gallium(III) complex is certainly too fast to follow with this technique. The slower rate of interconversion seen here for the tetrahedral hydroxamate cluster can be attributed to the geometric properties of the ligand and the cluster. In order for a metal center to change its chirality it is necessary to pass through a trigonal prismatic transition state. Since four coordination centers are tethered in the tetrahedron, the Bailar twist is the only mechanically possible rearrangement. This rearrangement requires that the coordinating ligands of the metal ion must pass through a conformation where the ligand's two coordinate vectors cannot lie in the chelate planes of each metal center. In effect, because the ligand maintains a coordinate vector angle of 60° in its planar form (Figure 1b), it forces a very distorted trigonal prismatic intermediate. Thus, *while the bimodal ligand can accommodate either hetero- or homochiral centers at both ends within the cluster, it fixes the chirality at each center once formed.*

The stereochemical course and potential energy diagram for the isomerization of the $\Delta\Delta\Delta\Delta$ to the $\Lambda\Lambda\Lambda\Lambda$ cluster is drawn in Figure 5. To isomerize from the $\Delta\Delta\Delta\Delta$ to the $\Lambda\Lambda\Lambda\Lambda$ form, the cluster has to go through each of the other stereoisomers. Since both NMR observations and MM2 calculations suggest that all isomers are very close in energy, they are drawn here at the same energy level. The potential energy diagram then can be simplified if we assume that isomerization of $\Delta\Delta\Lambda\Lambda$ to

$\Delta\Delta\Delta\Lambda$ will have the same energy barrier as further isomerization to $\Delta\Lambda\Lambda\Lambda$, since both processes require inversion of configuration at only one metal center. Similarly, the inversion from $\Delta\Delta\Delta\Lambda$ to $\Delta\Delta\Lambda\Lambda$ should have the same energy barrier as inversion of $\Delta\Lambda\Lambda\Lambda$ to $\Lambda\Lambda\Lambda\Lambda$.

Coalescence of the NMR resonances at 9.04 and 8.73 ppm, which belong to the C_3 isomer, was observed at 300 K. The activation barrier for the inversion of configuration of the C_3 isomer ($\Delta\Delta\Delta\Lambda$ or $\Lambda\Lambda\Lambda\Delta$) was calculated according to the formula $\Delta G^{\ddagger} = (1.914 \times 10^2)T_c(9.972 + \log T_c - \log \Delta\sigma)$[31] [where $\Delta\sigma = \sigma(H_1) - \sigma(H_2)$ and H_1 and H_2 are frequencies of nonequivalent protons at 220 K] and is 58 kJ mol⁻¹. The NMR resonances for the S_4 isomer, which at 220 K appear at 9.10 and 8.78 ppm, coalesce at 300 K, and the energy barrier related to the inversion of configuration of this isomer was similarly calculated. The value of 58 kJ/mol is identical to the energy barrier related to the inversion of conformation of the C_3 isomer. The absence of any significant difference in the free energy of activation between the three isomers is consistent with the presence of all three (T, C_3, S_4) and the equal energy of homochiral (e.g., $\Lambda-\Lambda$) or heterochiral ($\Lambda-\Delta$) pairs of vertices connected by the bis-hydroxamate ligand. In contrast, the gallium helicate complex formed from a rigid bis catecholate ligand was found to be relatively strongly coupled, with the homochiral ($\Delta\Delta$ or $\Lambda\Lambda$) isomer about 23 kJ/mol lower in energy than the heterochiral ($\Lambda\Delta$) isomer.[22] The inversion barrier for the catechol helicate is 79 kJ/mol, significantly higher than the 58 kJ/mol observed for the hydroxamate tetrahedral cluster. That in turn is much higher than the barrier for inversion of a single tris-hydroxamate gallium complex: the coupling of the vertices markedly increases the transition state free energy for inversion of the vertices but does not affect the relative energies of the individual isomers (Figure 5).

Summary

The cluster-forming bis-hydroxamate ligand described here can adapt to the geometric requirements of a M_4L_6 cluster in two ways: one in which the ligand spans metal ions of like chirality and one in which it spans metals of opposite chirality. The solid-state structure of the cluster and MM2 calculations indicate that these two structural forms of the ligand are not significantly different, with only the relative direction of two torsion angles distinguishing them. Because the two ligand forms lead to virtually no disruption to the metal−metal distance in the cluster, each arm of an individual ligand can be considered to be essentially independent of the other. Quantitative NMR studies have shown that all of the possible isomers are present in solution in a nearly statistical distribution. The various stereoisomers all form and interconvert, with the activation barrier for interconversion identical for all stereoisomers. However, the ligand structure does inhibit a dissociative or trigonal twist path required for the $\Delta \leftrightarrow \Lambda$ interconversion. Therefore the isomerization is much slower than in simple tris-hydroxamate complexes, with a barrier $\Delta G^{\ddagger} = 58$ kJ/mol.

Experimental Section

Physical Measurements. The ¹H NMR spectra were recorded on a Bruker AMX 300 spectrometer. Microanalyses were performed by the Analytical Services Laboratory, College of Chemistry, University of California, Berkeley. Fast atom bombardment and electrospray mass spectra were obtained at the Mass Spectrometry Laboratory at the

(29) *CAChe, 3.6*; Oxford Molecular Group, Inc., Tektronix, 1991. The geometry at the metal center is fixed, using known structures. Hence only the ligand components require force field values.

(30) Caudle, T. M.; Crumbliss, A. L. *Inorg. Chem.* **1994**, *33*, 4077.

(31) Sandstrom, J. *Dynamic NMR Spectroscopy*; Academic Press: New York, 1982.

Supramolecular Tetrahedral M₄L₆ Cluster

J. Am. Chem. Soc., Vol. 121, No. 17, 1999 4205

University of California, Berkeley. Unless otherwise noted, all chemicals and starting materials were obtained commercially and used without further purification. Organic solvents and mineral acids were of reagent grade and were used as supplied. Tetrahydrofuran (THF) was distilled from sodium benzophenone prior to use. Water was deionized and further purified by a Millipore cartridge system (resistivity 18 MΩ cm). Metal complex syntheses were performed under a nitrogen atmosphere using Schlenk techniques.

Isophthaloyl Dichloride. Isophthalic acid (4.00 g, 24.1 mmol) was heated with 5 mL of $SOCl_2$ and a drop of DMF until gas evolution ceased. Excess $SOCl_2$ was then removed under reduced pressure. The liquid residue crystallized upon cooling to room temperature to yield a white crystalline product. Yield: 4.8 g (98%). ^{1}H NMR (300 MHz, $CDCl_3$): δ 8.80 (t, 1H, J = 1.8 Hz), 8.39 dd, 2H, J = 7.9 Hz, 1.8 Hz), 7.74 (t, 1H, J = 7.9 Hz).

N-(4-Methylphenyl)hydroxylamine. 4-Nitrotoluene (12.0 g, 87.5 mmol) was dissolved in a mixture of 5.0 g (94 mmol) of NH_4Cl, 100 mL of H_2O, and 100 mL of ethanol. Zinc powder (17 g, 260 mmol) was added to the mixture in small portions while the temperature was kept below 10 °C by cooling with an ice bath. After the addition of zinc was complete the mixture was stirred for 2 h and filtered. The precipitate was washed with ethanol, and the combined solvents were reduced by rotary evaporation. The resulting yellow solids were dissolved in diethyl ether, dried with $MgSO_4$, and filtered. The ether was removed by rotary evaporation. The resulting yellow residue was washed with hexanes to yield a white, flaky product. Yield :7.3 g, 67%. ^{1}H NMR (300 MHz, $CDCl_3$): δ 7.09 (d, 2H, J = 6 Hz), 6.92 (d, 2H, J = 6 Hz), 5.47 (bs, 2.5 H), 2.31 (s, 3H). Anal. Calcd (Found) for C_7H_9NO: C, 68.26 (69.20); H, 7.37 (7.24); N, 11.37 (11.56).

Isophthal-di-N-(4-methylphenyl)hydroxamic Acid (H₂E). To a solution of 6.1 g (50 mmol) of N-(4-methylphenyl)hydroxylamine in 40 mL of dioxane was added 4.0 mL (50 mmol) of pyridine. To the resulting mixture was added a solution of 5.0 g (25 mmol) of isophthaloyldichloride dropwise, while the temperature of the mixture was maintained below 15 °C. The mixture was stirred for 3 h. The solvents were removed by rotary evaporation, and the solid residue was treated with 100 mL of concentrated aqueous NH_3. After being stirred for 1 h, a white precipitate had formed and the mixture was filtered. The solid was stirred with 0.1 M HCl, washed with H_2O, and dried under vacuum to yield 4.2 g (44%). ^{1}H NMR (300 MHz, $CDCl_3$): δ 7.63 (s, 1 H), 7.35 (d, 2 H, J = 7.5 Hz), 7.12 (t, 1 H, J = 7.5 Hz), 7.10 (d, 4 H, J = 8.3 Hz), 7.02 (d, 4 H, J = 8.3 Hz), 2.33 (s, 6 H). Anal. Calcd (Found) for $C_{22}H_{20}N_2O_4 \cdot {}^1/_2(H_2O)$: C, 68.56 (68.30); H, 5.49 (5.10); N, 7.27 (7.40).

Fe₄(E)₆. To a solution of 200 mg (0.53 mmol) of H₂E and 2 drops of triethylamine in 30 mL of acetone was added a solution of 125 mg of Fe(acac)₃ (acac = acetylacetonate) (0.35 mmol) in 10 mL of acetone. The combined solutions were heated overnight, and a red microcrystalline precipitate formed. The solid was collected by filtration, washed with a small amount of acetone, and dried. Yield: 130 mg (68%). Anal. Calcd (Found) for $C_{132}H_{108}N_{12}Fe_4O_{24}(H_2O)_4$: C, 62.37 (62.12); H, 4.60 (4.98); N, 6.61 (6.21). FAB(+): MH$^+$ 2470.

Ga₄(E)₆. To a solution of 200 mg (0.53 mmol) of H₂E and 2 drops of triethylamine in 30 mL of acetone was added a solution of 125 mg of Ga(acac)₃ (0.35 mmol) in 10 mL of acetone. The combined solutions were heated overnight and gave a colorless microcrystalline precipitate. This was collected by filtration, washed with a small amount of acetone, and dried. Yield: 130 mg (68%). ^{1}H NMR (300 MHz, $CDCl_3$): δ 8.89 (1 H, s), 7.21 (4 H, d, J = 8.2 Hz), 7.06 (4 H, d, J = 8.2 Hz), 6.81 (2 H, d, J = 7.4 Hz), 6.61 (1 H, t, J = 7.4 Hz), 2.29 (6H, s). FAB(+): MH$^+$ 2524.

Large crystals of Ga₄E₆·DMF formed after adding the metal solution to a solution of the ligand and triethylamine in DMF and keeping the mixture at ambient temperature for a few days.

X-ray Crystal Structure of Ga₄E₆. The compound Ga₄E₆·18 DMF crystallizes in the tetragonal space group $I4_1/a$, with $Z = 8$ (Table 1). All measurements were made on a Siemens SMART diffractometer[32] with graphite monochromated Mo Kα radiation. Area detector frames

---

Table 1

empirical formula	$C_{186}H_{234}Ga_4N_{30}O_{42}$
formula weight	3840.91
crystal color, habit	colorless, prism
crystal dimens (mm)	$0.10 \times 0.10 \times 0.05$
crystal system	tetragonal
space group	$I4_1/a$ (no. 88)
Z	8
lattice params	$a = b = 24.0738(2)$ Å
	$c = 68.5828(5)$ Å
	$V = 39747.0(5)$ Å^3
D_{calcd} (g/cm^3)	1.284
F_{000}	16160
μ(Mo Kα) (mm^{-1})	6.18
diffractometer	Siemens SMART
radiation	Mo Kα ($\lambda = 0.71069$ Å)
	graphite monochromated
crystal-to-detector distance (mm)	60
temp (°C)	-103
scan type	ω (0.3° per frame)
scan rate (s/frame)	30
no. of reflns measd	total: 63804
	unique: 7710 ($R_{int} = 11.3\%$)
corrections	Lorentz−polarization
	absorption: ($T_{max} = 0.894$, $T_{min} = 0.774$)
structure solution	direct methods SHELXTL
refinement	full-matrix least-squares
function minimized	$\sum w(|F_o| - |F_c|)^2$
least-squares weights	$w = 1/\sigma^2(F_o^2) = 4F_o^2/\sigma^2(F_o^2)$
p-factor	0.030
anomalous dispersion	all non-hydrogen atoms
no. of observns ($I > 3.00\sigma(I)$)	7710
no. of variables	576
refln/param ratio	13.4
residuals: R; $R2_w$; R_{all}	0.089, 0.22, 0.12
goodness-of-fit indicator	1.085
max shift/error in final cycle	0.061
maximum peak in final diff map (e$^-$/Å^3)	0.58
minimum peak in final diff map (e$^-$/Å^3)	-0.53

---

corresponding to an arbitrary hemisphere of data were collected using ω scans of 0.3° and a total measuring time of 30 s each. Data were integrated using SAINT[33] with box parameters of $1.3 \times 1.3 \times 0.4°$ to a maximum 2θ value of 46.5°. The data reprocessing and subsequent refinement led to a significantly more accurate structure than reported in the preliminary communication.[15] An empirical absorption correction based on the measurement of redundant and equivalent reflections and an ellipsoidal model for the absorption surface was applied using XPREP.[34] Initially solved by direct methods using the teXsan software package,[35] the final structure solution and refinement were performed using the SHELXTL software package.[36] The Laue group is $4/m$ but twinned toward $4/mmm$. The twinning was modeled using the method of Pratt, Coyle, and Ibers.[37] The fractional contributions of the two twin components (related by $hkl−khl$) were refined to 25.2 and 74.8%. Four solvent molecules were found in the asymmetric unit, and the others are severely disordered. The solvent to cluster stoichiometry was derived from a ^{1}H NMR spectrum of crystals dissolved in acetone. Final cell parameters are in Table 1, while atom coordinates and isotropic thermal parameters are as CIF files (Supporting Information).

(32) *SMART Area-Dectector Software Package*; Siemens Industrial Automation, Inc., Madison, WI, 1995.

(33) *SAINT: SAX Area-Detector Integration Program, V4.024*; Siemens Industrial Automation, Inc., Madison, WI, 1995.

(34) *XPREP, 5.03*; Siemens Industrial Automation, Inc., Madison, WI, 1995.

(35) *teXan: Crystal Structure Analysis Package*; Molecular Structure Corp., 1992.

(36) *SHELXTL Crystal Structure Analysis Package*; Siemens Industrial Automation, Inc., Madison, WI, 1995.

(37) Pratt, C. S.; Coyle, B. A.; Ibers, J. A. *J. Chem. Soc. (A)* **1971**, 2146.

Supporting Information Available: Complete details of the structure solution and refinement, including atom coordinates, isotropic and anisotropic thermal parameters, bond distances, and bond angles, are available in CIF format. This material is available free of charge via the Internet at http://pubs.acs.org.

JA984046S